Combustion and Flame 220 (2020) 235–246

Contents lists available at ScienceDirect

Combustion and Flame

journal homepage: www.elsevier.com/locate/combustflame

# Experimental study of the effect of C8 oxygenates on sooting processes in high pressure spray flames

Irene Ruiz-Rodriguez [a,*], Roger Cracknell [b], Michael Parkes [b], Thanos Megaritis [a], Lionel Ganippa [a]

[a] Mechanical, Aerospace and Civil Engineering Department, Brunel University London, UB8 3PH, United Kingdom
[b] Shell Global Solutions, Shell Centre, 4 York Road, Lambeth SE1 7NA, United Kingdom

ARTICLE INFO

*Article history:*
Received 10 September 2019
Revised 6 June 2020
Accepted 8 June 2020
Available online 15 July 2020

*Keywords:*
Oxygenates
Soot
Combustion fundamentals
Constant volume chamber

ABSTRACT

Oxygenated compounds have the ability to reduce soot emissions and to improve the combustion efficiency in engines. Most studies have focused on the soot reduction potential of shorter carbon chain oxygenates, whilst longer carbon chain oxygenates are still relatively unexplored. In this work, the soot reduction potential of long carbon chain oxygenates having similar thermo-physical and chemical properties to those of diesel have been studied, viz., 2-octanone (ketone), 1-octanol (alcohol), hexyl acetate (ester) and octanal (aldehyde). These oxygenates were injected at high pressure into a constant volume chamber maintained at high ambient temperature conditions, and their spray flames were investigated using a high-speed, two-colour pyrometry system. It was found that for the same injected fuel mass, the oxygenates reduced the overall soot when compared to diesel. Small differences in sooting tendencies were observed between different oxygenated moieties but these were smaller than those relative to diesel. The absence of aromatic groups and the presence of oxygen directly bonded to carbon atoms seemed to have a larger effect on soot reduction than the oxygenated functional group. The oxygenates altered the local oxygen equivalence ratio in the spray, influencing the soot formation and its distribution in the flame. Under the high pressure conditions studied, the average sooting tendency of the long carbon-chain oxygenates studied increased in the order of: ester< aldehyde ~ alcohol<ketone.



## 1. Introduction

Modern diesel engines have to comply with increasingly stringent controls on emissions. Soot emissions are generally controlled by the use of a diesel particulate filter (DPF), but the effect of increased back pressure and frequent regeneration of DPFs adversely affects fuel economy [1]. Additionally, soot can also cause oil dilution, leading to issues with lubrication [2]. One approach to reduce engine-out soot is to improve the in-cylinder combustion process by fuelling with oxygenated fuels. Several studies have shown that the use of short carbon chain oxygenates can reduce soot emissions [4–9]. Whilst these outcomes are promising, short carbon chain oxygenates do not necessarily match the energy content of diesel, so long carbon chain oxygenates that could be candidates for blending with diesel must also be explored. Data on the fundamental combustion characteristics of long carbon chain oxygenates under engine-like conditions are still lacking, and there is a need to understand their combustion characteristics to explore their potential as low-carbon design fuels.

Studies in burners, constant volume chambers and engines have demonstrated that for the same amount of oxygen in the fuel, the molecular structure does have some effect on soot formation [3–7]. The oxygen extended sooting index (OESI) was used in [6] to quantify the sooting tendency of oxygenates with different functional groups using a smoke point lamp. The study revealed that for a given carbon number, the sooting tendency increases in the order of aldehydes<alcohols<ketones<ether. On the other hand, in [9], the sooting trends in turbulent flames of different oxygenates blended with a diesel surrogate showed an increase in the order of: aldehydes<ketones<alcohols. In [10], the sooting propensity of dimethyl ether, acetone, butanal, and 3-pentanone in n-heptane/oxygen mixtures was studied in a shock tube. It was reported that aldehydes were the most effective compound for soot reduction, followed by ketones and esters. They also reported that increasing the n-alkyl carbon chain length from ace-

* Corresponding author.
*E-mail address:* irene.ruizrodriguez@brunel.ac.uk (I. Ruiz-Rodriguez).

https://doi.org/10.1016/j.combustflame.2020.06.015

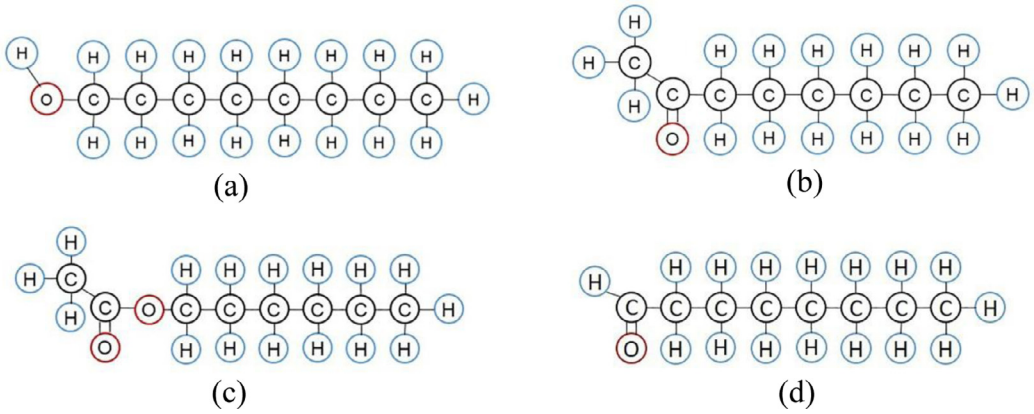


**Fig. 1.** Chemical structure of the oxygenated fuels studied: (a) 1-octanol, (b) 2-octanone, (c) hexyl acetate, (d) octanal.

tone to 3-pentanone did not have a significant effect on soot formation, which implies that for the compounds investigated, the effect of oxygen content on soot formation is greater than that of the n-alkyl carbon chain length. In [11], the sooting tendency of several oxygenates was studied by doping methane/air non-premixed flames with each test oxygenate. It was reported that for the oxygenates, soot processes were influenced by the carbon chain length, the molecular structure of each fuel, and also by the location of the oxygen atom within the carbon chain of a compound.

Despite numerous works reporting on the effect of oxygenates on sooting propensity, the effect and extent of different oxygenate moieties on soot reduction is still unclear. It has been suggested that the length and the complexity of the oxygenate chain affects the production of soot precursors [5], and thus overall soot emissions. Some numerical studies, for example [12,13], have explored the chemical reaction pathways of molecular oxygen in different functional groups, and have shown that they have different soot reduction efficiencies, which are attributed to how the oxygen reacts and how it affects the partial pyrolysis of the fuel and the concentration of radicals. In [12], they showed that ethanol, dimethyl ether, dimethoxy methane, and methyl butanoate reduce the formation of soot precursors at a similar rate but the efficiency of the ester group in doing so is less due to the capture of the carbon by two oxygen atoms to form $CO_2$. This would imply that besides the effect of dilution, which is the replacement of high-sooting molecules such as aromatics by less sooting ones such as aliphatics, the effect of the different functional group is, to some extent, important for soot reduction. In [13], a new model was developed based on machine learning algorithms to determine the effects of the functional group and the chemical structure on sooting propensity of oxygenates. They determined that both the oxygen functional group and the carbon chain structure have an effect on the sooting propensity, and that the extent of these effects were different depending on the type of oxygenate. These numerical studies provided a valuable insight into the detailed chemical mechanisms and the sooting propensity of different oxygenates.

The combustion characteristics of di-n-butyl ether (DNBE) and n-octanol were investigated in [14,15], where it was concluded that the fuel-bound oxygen affects the local stoichiometry and ignition characteristics, which in turn influence the overall engine combustion and emission performance. They showed that DNBE and diesel produced a similar amount of soot due to DNBE's prompt ignition and short lift-off length leading to a reduced level of mixing. On the other hand, n-octanol reduced soot emissions due to its higher degree of pre-mixing. Decomposition pathways of DNBE were further explored in [16,17]. In [18], the ignition and emission properties of various C8-C16 compounds were investigated using a research engine and a gas analyser. They showed that the emissions were dependent on the functional group and on the effect that the compound had on the ignition delay. These studies provided interesting data under engine-like conditions and showed promising outcomes, but to date, there are few optical studies that characterise the combustion and flame fundamentals of long carbon chain oxygenates. Optical characterisation of the flames is important to understand the fundamentals of soot formation and oxidation, and to provide combustion data on potential drop-in fuels.

This study aims to address this gap by exploring the combustion fundamentals of different C8 oxygenated fuels (1-octanol, 2-octanone, hexyl acetate, and octanal) and diesel in an engine-like environment at high ambient temperatures and low ambient oxygen concentrations. This work provides insights into the spatio-temporal evolution of soot in spray flames for the full duration of the combustion event, and it also provides a relative comparison of the soot reduction attained by each fuel. These fuels have been selected because of their thermo-physical properties and also due to the promising advances in their production methods [19–21]. Furthermore, very little information is available on the combustion characteristics of hexyl acetate and 2-octanone. The fuels were injected at a high pressure in a constant volume chamber and the filtered natural luminosity was imaged using a high-speed two-colour pyrometry system to obtain the flame soot and temperature distributions. The variation in the sooting propensity and distribution between the functional groups has been elucidated, however, the exact chemical mechanisms that cause soot reduction are not clear.

In the following section, Section 2, a description of the fuels used is provided alongside a description of the experimental methods. In Section 3, the combustion properties of the oxygenates and the spatio-temporal distributions of soot and temperature are discussed. Finally, a set of conclusions is provided with a summary of the main findings.

## 2. Experiments

### 2.1. Fuels

The oxygenates studied were C8 linear compounds: 1-octanol (alcohol), 2-octanone (ketone), hexyl acetate (ester) and 1-octanal (aldehyde), with chemical structures as shown in Fig. 1. 1-Octanol has a hydroxyl group (-OH) linked to the first carbon site via a single bond (Fig. 1(a)); 2-octanone is characterised by the carbonyl group (C=O) next to the methyl group (Fig. 1(b)); hexyl acetate contains the distinctive carboxyl group (C(=O)OH) with the hydrogen substituted by an alkyl group (Fig. 1(c)); and octanal has a C=O group with a hydrogen attached at one end of the carbonyl

**Table 1**
Thermo-physical properties of the fuels studied. [a][22], [b][23], [c][24], [d]Calculated property, [e][14], [f][68], [g]Product's chemical sheet or SDS, [h][26], [i][25], [j][27], [k][28], [l][29], [m][30]. *DCN.

| Fuel | Diesel | 1-Octanol (1-OL) | 2-Octanone (2-ONE) | Hexyl Acetate (HA) | Octanal (OAL) |
|---|---|---|---|---|---|
| Density (kg/m$^3$) | 850[a,g] | 824[e] | 819[g] | 870[g] | 821[g] |
| Lower calorific value (LCV) (MJ/kg) | 43[b] | 38[g] | 40[d] | 37[d] | 40[d] |
| Cetane number | 48[g] | 39[f] | 37[f,*] | 32[f,*] | 80[i] |
| Boiling point (K) | >438[g] | 467[g] | 447[g] | 445[g] | 444[g] |
| Auto-ignition temperature (K) | 553[c] | 567[g] | 568[g] | 528[h] | 463[i] |
| Flashpoint (K) | 329[g] | 353[g] | 329[g] | 328[g] | 325[g] |
| Heat of vaporisation (kJ/kg) | 270[j] | 502[k] | 405[l] | 362[m] | 420[m] |
| C/O | N/A | 8 | 8 | 4 | 8 |
| H/C | N/A | 2.25 | 2 | 2 | 2 |

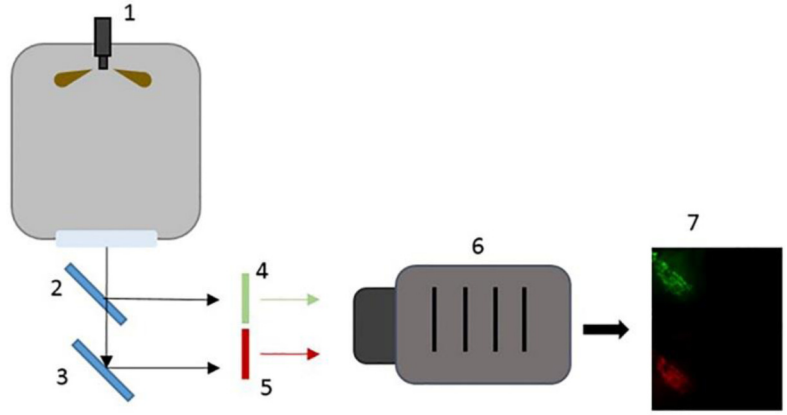


**Fig. 2.** Simplified experimental set-up schematic including: 1. Injector, 2. 50–50 Beam splitter, 3. Mirror, 4. 543.5 nm filter, 5. 670 nm filter, 6. High speed camera and 7. Sample image of the collected data.

group. The corresponding thermo-physical properties of these oxygenates are shown in Table 1.

The density, calorific value, boiling point, and autoignition temperature are similar for all the fuels studied, but the difference in volatility and chemical composition yields a different cetane number for the fuels. Amongst the oxygenated fuels considered, octanol, octanone, and octanal have the same C/O ratio of 8, but a different H/C ratio of 2.25 for octanol and 2 for octanone and octanal. For hexyl acetate, even though its H/C ratio is the same as that for octanone and octanal (H/C = 2), its C/O ratio is 4, which is different from the other oxygenates. These differences in molecular composition allowed for the exploration of the effects of both H/C and C/O ratios on the sooting propensity of the fuels. All the fuels discussed were tested in this work except for octanal, for which the data were obtained from [31] and is discussed in Section 3.1.

### 2.2. Set-up and operating conditions

All fuels were injected neat into a high-pressure, high-temperature environment in an optically accessible constant volume chamber (CVC) maintained at an ambient temperature of ~1300 K and an ambient pressure of ~35 bar. This facility allows for a high controllability of the ambient temperature and pressure. The chamber conditions were obtained by burning a lean mixture of $C_2H_2$ and air, with relative partial pressures of 3.9% and 96.1%, resulting in an unburnt oxygen concentration of ~10%. It has been used extensively in the literature, and more details of its operation and design can be found in [32,33]. The fuels were injected at 700 bar by means of a six-hole solenoid actuated common rail injector, managed by an automated control unit. At least seven injections were performed per fuel, and the injection duration was adjusted for each oxygenate to match the mass of diesel injected during an injection time of 1.5 ms. The combustion events were acquired using a high-speed CMOS camera operated at 18 kfps (kilo frames per second), with an imaging area of 768 × 960 pixels$^2$, a resolution of 90 µm per pixel and an exposure time of 54.54 µs. To maximise the spatial resolution, only one of the six spray flames was imaged in the CMOS detector. In order to implement the two-colour method, a beam splitter and a mirror were used alongside two narrow band-pass filters placed in front of the detector, as shown in Fig. 2, to acquire two wavelength-specific images of the same flame. The filters used were centred at wavelengths of 543.5 nm ($\lambda_1$) and 670 nm ($\lambda_2$), with a full width half maximum (FWHM) of 10 nm to minimise stray emissions reaching the sensor. The flame temperature and soot concentration were acquired using the two-colour pyrometry technique, which is detailed in Section 2.3.

### 2.3. Two-colour pyrometry

The two-colour (2C) pyrometry method is versatile and has been widely used by many researchers to characterise sooting flames [34–36]. It relates the radiation intensity emitted by the soot ($I_{soot}$) to its temperature ($T$) and to a variable proportional to the soot volume fraction ($K$) in terms of the optical path length ($L$) at a specific wavelength ($\lambda$). The combined value of $K$ and $L$ is referred to as the soot concentration or KL factor [37,38]. This 2C method is based on Plank's law, which relies on the radiation emitted by a black body ($I_B$), and on the emissivity ($\varepsilon$) of the imaged non-black body, which can be obtained through a semi-empirical relation [37]:

$$I_{soot}(\lambda, T, KL) = \varepsilon\ I_B(\lambda, \mathrm{T}) = \left[1 - \exp\left(-\frac{KL}{\lambda^{\alpha}}\right)\right] \frac{C1}{\lambda^5\left[\exp\left(\frac{C2}{\lambda \mathrm{T}}\right) - 1\right]} \quad (1)$$

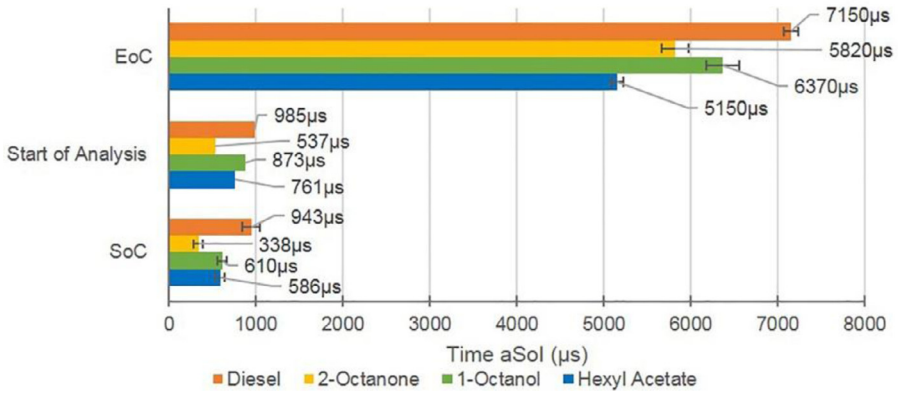


**Fig. 3.** The timings of the events related to the processes observed in the chamber, relative to the SoI – 0 in the graph.

where $\alpha$ is the dispersion coefficient, which was set to 1.39 [36,37,39]. The two constants $-C_1$ and $C_2-$ can be expressed as $C_1=2\pi hc^2$ and $C_2= hc/k$, where $h$ is Planck's constant, $c$ the speed of light in vacuum and $k$ the Boltzmann constant. To be able to solve for the unknowns ($T$ and KL), Eq. (1) requires radiation data for at least two wavelengths ($\lambda_1$ and $\lambda_2$). To obtain the soot radiance at every pixel location, the high-speed CMOS camera signal ($S_\lambda$) was related to the soot radiation through a calibration factor ($C_\lambda$) at the two wavelengths of interest, Eq. (2). The first step in the calibration procedure was to calibrate a tungsten halogen light source using an integrating sphere, to obtain the spectral radiant flux at different light intensities. Thereafter, the calibrated light source was positioned in the CVC, and images were acquired with the camera to capture the light intensity at different throughputs. This intensity was then used to obtain a relation between radiance values and camera pixel intensity.

$$I_{soot}(\lambda, \mathrm{T}, \mathrm{KL}) = C_\lambda S_\lambda \tag{2}$$

The 2C pyrometry method provides line-of-sight information of both the flame temperature and the soot distribution without perturbing the flame, and it is useful to obtain data on the relative variations in temperature and KL between fuels. The calculated KL value is subject to uncertainties due to set-up specific limitations, and due to the optical thickness of highly sooting regions yielding non-physical solutions. For the latter, flame pixel regions yielding non-physical solutions were solved by setting a limiting value to the emissivity of 0.994, set based on the wavelengths used in this work. This resulted in a maximum possible KL value of 2.95 for optically thick flame regions, which could reach up to 50% and 14% of the imaged area for diesel and the oxygenates respectively when the soot concentration was the highest. Similar observations have been reported in [34–36]. Even though the method's limitations constrain the treatment of soot concentration values to a semi-qualitative one, the analysis is robust and consistent for the purpose of relative comparison between fuels.

## 3. Results and discussion

The global in-cylinder combustion events studied in this work are presented in Fig. 3: the start of combustion (SoC), the end of combustion (EoC) and the time at which the data analysis was started. The data are presented relative to the time after the start of injection (aSoI). In this work, the SoC refers to the first appearance of soot, and in a similar manner, the EoC refers to the last appearance of soot. A Tukey test was performed on the SoC and EoC data to determine any statistical significant differences between the fuels [40]. This analysis provided confirmation that the differences between fuels were statistically significant with a 95% confidence level. The only exception was the difference in SoC between hexyl acetate and octanol, which did not present a statistically significant difference and thus have to be considered as equal. The start of analysis shown in Fig. 3 is the point in time at which the signal-to-noise ratio (SNR) was high enough to detect the flame for its analysis.

The first appearance of soot (SoC) in the spray was in the form of small soot pockets that were randomly distributed downstream of the nozzle tip, as shown in Fig. 4. These small pockets of soot were mostly short-lived, and eventually quenched as combustion proceeded. These small pockets of soot are thought to form from pockets of fuel that detach from the spray periphery due to its aerodynamic break-up when injected at high pressures into the CVC. The pockets at the spray periphery suffer loss of momentum and energy, so they are unable to mix with the ambient oxygen, becoming fuel-rich. This also means that the oxygen available was mostly fuel-bound. The presence of fuel-bound oxygen in the neat oxygenates could have led to a fast cracking and partial pyrolysis at the high ambient temperatures studied. It has been shown in previous works that adding small amounts of oxygen to the fuel can enhance pyrolysis, as a result of the fast accumulation of soot-forming radicals and precursors [41–44]. These short-lived soot pockets have also been observed in [45]. It was interesting to note that these soot pockets appeared first for octanone, followed by octanol and hexyl acetate, and finally by diesel.

As combustion proceeded and the localised soot pockets quenched, soot eventually stabilised slightly further downstream for the oxygenated fuels than for diesel (Fig. 5). This shows that the pockets of soot observed during the early injection stages were transient and did not impact the soot lift-off-length (LoL) significantly. The soot LoL was similar for the oxygenates studied, which suggests that for the oxygenates, the ambient conditions had a larger effect on soot stabilisation than any of the other fuel properties.

In this work, we have measured the soot LoL and not the flame LoL. Normally, the degree of premixing is reflected by the distance from the nozzle tip to the first appearance of OH chemiluminescence (flame LoL) rather than to the first appearance of soot luminosity (soot LoL). The degree of premixing was kept to a minimum by maintaining the ambient temperature in the chamber significantly higher than the autoignition temperature of each fuel, which forced each oxygenated fuel to have a similar flame stabilisation location. This is supported by the discussions in [46,47], where they demonstrate that for ambient temperatures above ~1100 K, the difference in flame LoL between different fuels becomes small, which minimises the differences in air entrainment due to pre-mixing. Since the flame LoL can be considered to be similar at high ambient temperatures, the degree of premixing and air entrainment can be considered to be comparable for all oxygenated fuels. Hence, the discussions hereafter on the differences between fuels will fo-

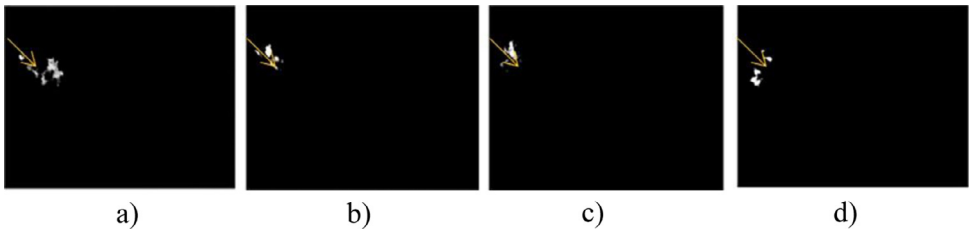


**Fig. 4.** Single shot images representative of the first appearance of soot for diesel and the oxygenates studied. The image brightness has been adjusted for visualisation purposes. The arrows show the approximate travelling direction of the spray, and the nozzle tip is located just out of the field of view towards the left-most corner: (a) diesel, 929 μs aSoI, (b) octanol, 593 μs aSoI, (c) octanone, 369 μs aSoI, (d) hexyl acetate, 537 μs aSoI.

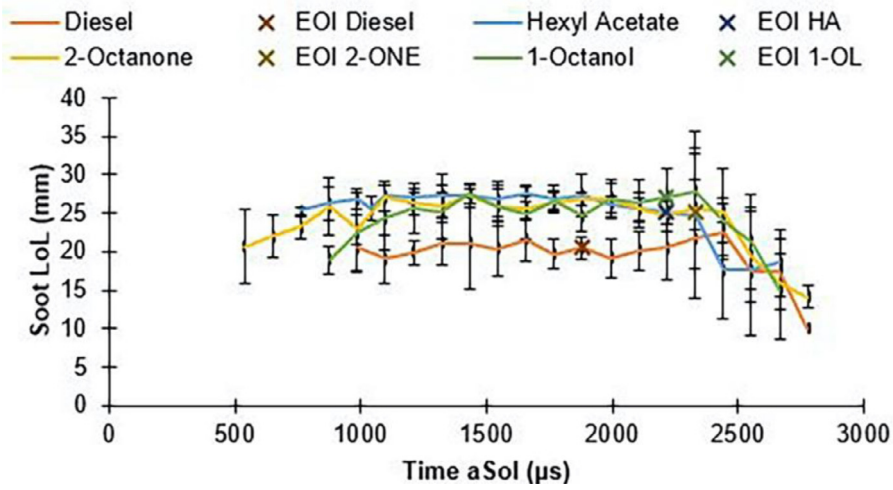


**Fig. 5.** Soot lift-off-length and corresponding end of injection (EoI) timings for all fuels.

cus on the chemical structure and composition of the fuels rather than on the pre-mixing effects.

Towards the end of combustion, soot oxidation reactions are important, as they reduce engine-out soot and also the load on after-treatment systems [48–50]. When looking at the EoC in Fig. 3, it can be seen that the hexyl acetate flame was the first to fully oxidise, followed by octanone, octanol and finally diesel. The details of the oxidation process will be discussed in the following sections.

### *3.1. Temporal variation of temperature and soot*

The spatial distribution of the temperature in the spray flame at each time instant was averaged over every flame pixel location for at least seven injections per fuel, and the results are shown in Fig. 6. A similar analysis was performed for the soot concentration, and this is shown in Fig. 7. The inset in Fig. 7 is the zoomed-in version of the soot distribution for the oxygenates only, shown for ease of visualisation.

During the initial phases of ignition, evaporative cooling effects tend to be significant, and this is reflected in the lower flame temperatures. For these initial reaction regions, it can be seen that the deviation was larger, which partly reflects the larger scatter in high and low temperature regions during this initial combustion phase. As the flame developed from its local ignition sites, the mean value of the spray flame temperature increased until it reached a constant value, which was on average similar for all the fuels studied. During the stable combustion period, the difference in the mean global flame temperature between fuels was negligible, which could be because of their similar LCVs. Towards the EoC, after the injection terminated, the remaining flame loses momentum as it decouples from the spray and forms corrugated islands of soot, which were oxidised during the late oxidation stages. As these remaining pockets of fuel products and soot were consumed, the flame temperature decreased for all fuels, with the fastest decrease experienced by those fuels which oxidised faster. Localised high and low flame temperature regions observed in the flame islands towards the final combustion stages caused the larger variations observed in the mean global temperature when compared to the stable combustion stage.

The results presented in Fig. 7 show that for all fuels, the soot formation initially dominated over the oxidation until the soot concentration reached a peak. Thereafter, the oxidation dominated the sooting processes and the average soot concentration decreased until all the soot was consumed. Even though this generic trend was similar for all fuels, the sooting propensity was different for the different fuels. The soot concentration for diesel was the largest, and after reaching the peak, it took the longest time to oxidise. Some differences were also observed in the sooting propensity between the oxygenates, however, the inset in Fig. 7 shows that the differences in sooting tendencies between oxygenated fuels were smaller than the differences between the oxygenates and diesel. This suggests that for the conditions studied, the dilution effect and decreasing the carbon chain length had a larger effect on soot reduction than changing the oxygenate moiety. Nonetheless, these small differences in sooting tendencies between oxygenates can be attributed to the differences in functional groups. For the oxygenates the sooting trend was, from the highest sooting fuel to the lowest, in the order of: 2-octanone>1-octanol>hexyl acetate. Based on the works of the references provided, hypotheses have been proposed to explain the observed soot reduction trends for the different C8 oxygenated moieties.

When comparing octanone to diesel, besides the effect of the absence of aromatics and the shorter carbon backbone on soot reduction, the presence of the carbonyl oxygen (=O) in octanone has been shown to irreversibly trap the carbon due to its rel-

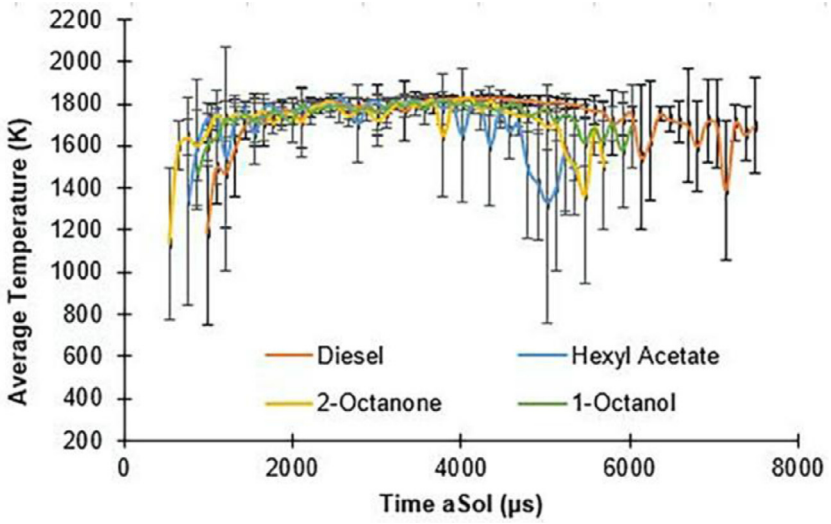


**Fig. 6.** Temporal evolution of the temperature for the fuels studied. The error bars cover two standard deviations from the mean.

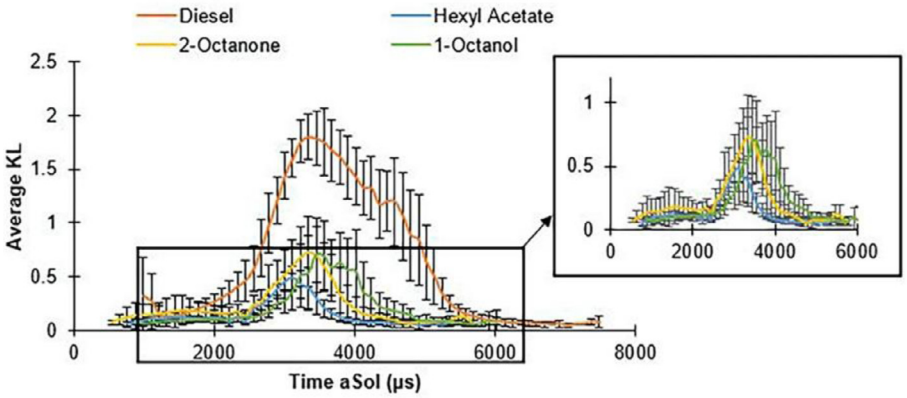


**Fig. 7.** Temporal evolution of the soot for the oxygenated fuels studied and a zoomed-in section of the oxygenates. The error bars cover two standard deviation from the mean.

atively high bond dissociation energy (BDE), inhibiting some reaction pathways that lead to soot-forming reactions [11]. On the other hand, when comparing octanone to the other oxygenates (1-octanol and hexyl acetate), it was observed to soot slightly more, and this could also be related to the presence of the C=O bond that can allow for more electron de-localisation [18], which can lead to the formation of stable radicals, favouring the formation of soot precursors [52]. In addition to this, the methyl group attached to the carbonyl bond in octanone is relatively weak compared to the C=O, and can break away from the parent molecule. This can promote the formation of methyl radicals that enhance the formation of propargyl and other soot precursors, which serve as building blocks for soot [53,54]. The secondary carbon next to the carbonyl group could also undergo beta-scission, as the BDE of the C–C bond is relatively low [51,55,56], which would promote the formation of longer alkyl chain radicals. Other decomposition pathways could also be playing a role, as the molecule size is large. Furthermore, once a bond breaks, the effect it has on the remaining bonds and subsequent decomposition pathways can be complex [57]. For these reasons, the proposed reaction pathways must be treated as hypotheses, as only chemical kinetic models would be able to provide quantitative data on the likelihood of the aforementioned routes. Overall, the net effect of these chemical pathways was to reduce the amount of soot octanone produced when compared to diesel but to increase it slightly when compared to the other oxygenates studied. The former soot reduction effect when compared to diesel was larger than its enhancement when compared to the oxygenates, which implies that dilution effects had a stronger effect on soot reduction capabilities than moiety-specific effects.

For alcohols, its soot reduction effect when compared to diesel has been previously attributed to dilution effects rather than to moiety-specific effects [11]. This is because the hydroxyl (-OH) group has a strong BDE and inhibits the oxygen atom from linking to a carbon, which does not favour a reduction in soot formation. The decomposition pathways for octanol have been presented for example in [58], however, it has also been shown that the decomposition pathways of short carbon-chain alcohols can be used as a starting point to understand the decomposition of longer carbon-chain alcohols. Literature studies on lower carbon-chain alcohols such as butanol or propanol have shown that alcohols can decompose via several pathways, and besides H-abstraction and simple fission, complex fission can occur via four-centre elimination pathways that lead to dehydrogenation and the production of an alkene [11,59–61]. This could be one of the routes leading to soot formation in octanol. When compared to octanone and hexyl acetate, octanol took the longest to reach its soot formation peak. As combustion advanced, its peak was observed to be just under octanone, but 200 μs after. For octanol, the net effect when compared to diesel was a reduction in soot. Based on the known

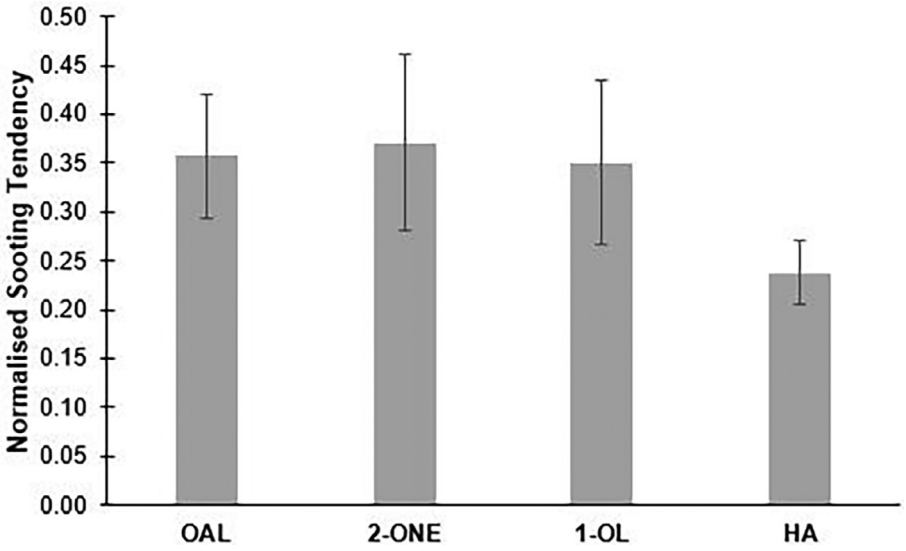


**Fig. 8.** Sooting tendencies for the fuels studied in this work and for octanal (aldehyde), relative to diesel. The error bars cover one standard deviation.

and previously established reaction pathways discussed in this section, our results also indicate that dilution effects are the dominant reasons for soot reduction. Its chemical structure only had a small effect on its soot reduction potential under the high pressure and temperature conditions studied when compared to octanone.

Out of all the investigated C8 linear oxygenates, hexyl acetate produced the least amount of soot. Even though it produced least amount of soot, it attained a relative soot reduction of ~10% compared to the other oxygenates (based on KL in Fig. 7), despite the fact that it had half the C/O ratio. Whilst only little information is available on the cracking of hexyl acetate, it is known that the C=O and C–O bonds in the ester groups have higher BDEs than their surrounding bonds, which causes the C atom to strongly bond to the oxygen atoms and form $CO_2$ [5,62,63]. Thus, it results in an ineffective use of oxygen despite producing the least amount of soot. This also suggests that the soot reduction potential of hexyl acetate is governed by dilution rather than moiety-specific effects, similar to the other oxygenates studied.

All oxygenates oxidised faster than diesel, an observation which is consistent with the results in [64–66], where they found that compounds with fuel-bound oxygen produced soot that was more readily oxidised due to its more amorphous structure and higher tortuosity level. The soot produced from the combustion of hexyl acetate oxidised the fastest, followed by octanone and octanol. It is known that soot reactivity and its oxidation depends on the physical and chemical properties of soot [67], so the differences in oxidation observed in Fig. 7 between oxygenates could be caused by the differences in the chemical characteristics of the produced soot. It could also be that because the oxygenates produced less soot, there was less soot that needed oxidising and thus it would take less time for it to oxidise than diesel.

In addition to the aforementioned oxygenates, the sooting tendency of a C8 oxygenate with an aldehyde moiety, octanal, that was studied by the authors in [31] has been incorporated to this work for comparison with the rest of the C8 oxygenates. As discussed in [31], besides dilution effects, the reduction in sooting propensity of octanal was attributed to the presence of oxygen in the carbonyl group (C=O) inhibiting the participation of the carbonyl C atom in any soot forming reactions. A comparison of the sooting tendency of all oxygenates relative to diesel is shown in Fig. 8. These data have been obtained by taking the average value of the KL factor in the flame for each time instant, and further taking the time average for the complete combustion event to obtain a single mean representative value. The difference in the temporally averaged KL factor for the oxygenates was normalised with diesel to compare the sooting reduction potential of each oxygenate against diesel. From the graph, it can be seen that the average soot yield decreased in the order of: ketone>aldehyde~alcohol>ester, which shows that the ester group still has the largest sooting reduction potential. However, when accounting for the C/O ratio it seems that the alcohol and the aldehyde are more efficient at reducing global soot than any of the other moieties. Furthermore, because the fuels were injected into a high ambient temperature environment, the effects due to the different CN of the fuels was not expected to have any significant impact on the ignition and sooting propensity.

The observed reductions in sooting potential of the moieties studied in this work are similar to those in [6,9] with respect to ketones and aldehydes; as well as ketones and alcohols in [6]. However, some discrepancies were noted in [6] regarding the sooting order between the aldehyde and the alcohol, where the latter showed a higher tendency to soot than the former, whereas in our work both alcohol and aldehyde had a similar sooting tendency. The differences in the sooting trend between the alcohol and the aldehyde in [6] and in our work could be related to an increase in the carbon chain length from C5 to C8. As the carbon chain length increases, the effect of the moiety relative to the effect of the carbon chain length on sooting propensity tends to decrease, so the differences between the alcohol and the aldehyde moieties were minimised. With respect to the sooting tendencies for the ketone and the alcohol, we observed a reverse trend to that reported in [8,9]. These discrepancies can also arise because of the differences in ambient conditions and test fuels, as in this work, neat oxygenates were studied under a high-pressure, high-temperature environment. This raises an important point: even though the underlying chemical mechanisms for molecule break-down might remain unchanged, other effects such as flame type, ambient conditions, mixing, entrainment and carbon chain length can modulate the sooting propensity of the different moieties.

The results presented in this section revealed that relative to diesel and for the ambient conditions studied, fuelling with neat C8 oxygenates reduces the overall soot formation and also enhances its oxidation without altering the global flame temperature.

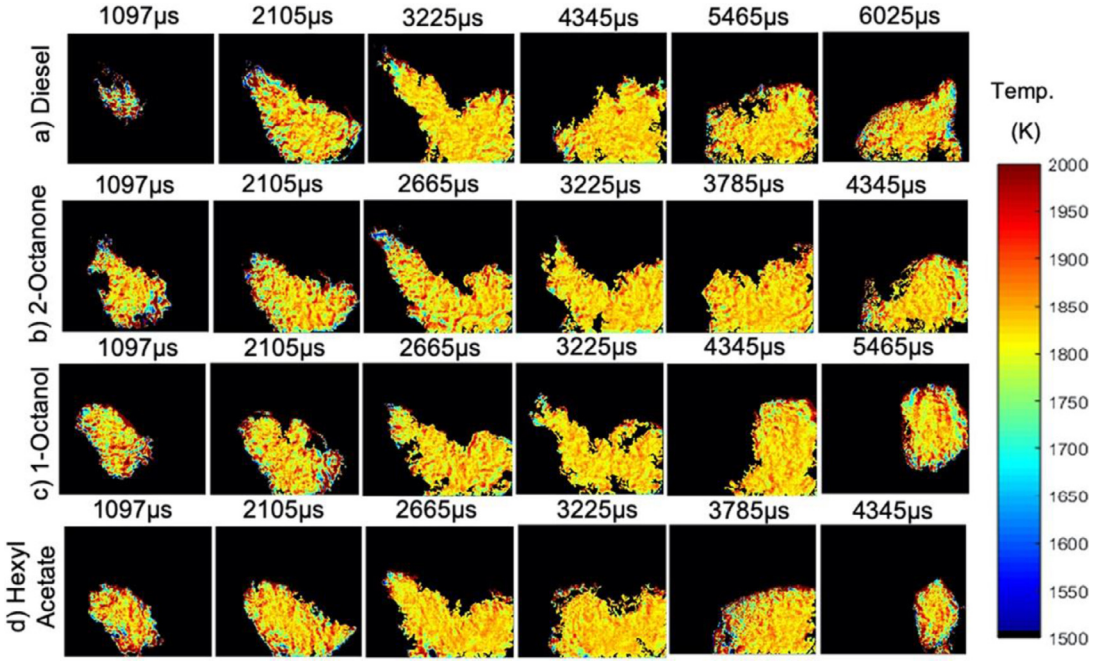


**Fig. 9..** (a–d) Spatial distribution of the temperature for: (a) diesel, (b) 2-octanone, (c) 1-octanol, (d) hexyl acetate.

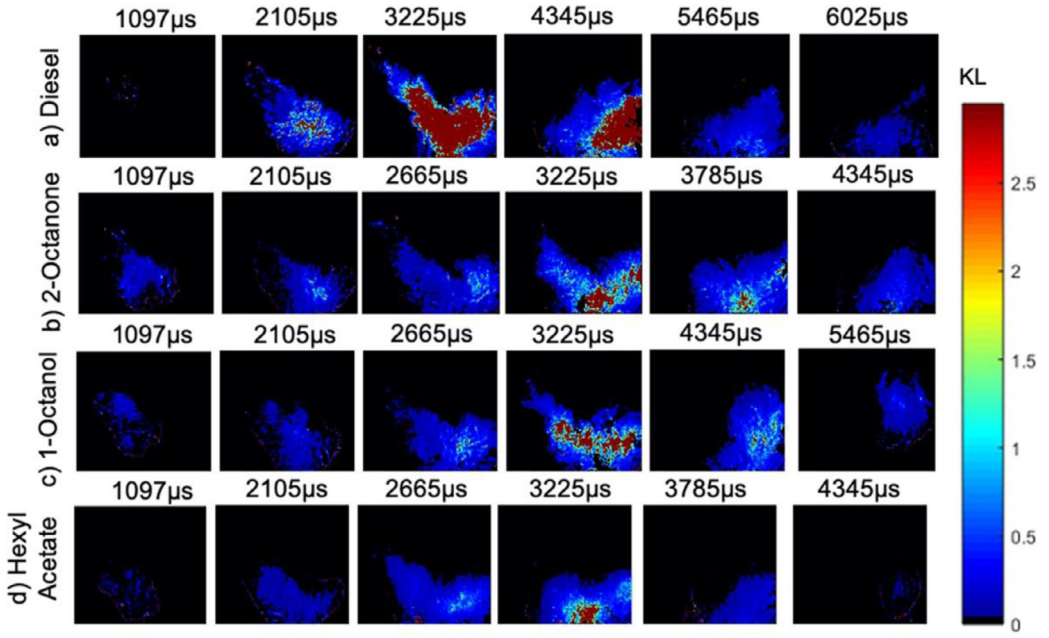


**Fig. 10..** (a–d) Spatial distribution of the soot for: (a) diesel, (b) 2-octanone, (c) 1-octanol, (d) hexyl acetate.

Furthermore, the moiety-specific effects do play a role in soot suppression but to a much lesser extent than dilution effects (i.e. chain saturation, chain length and aromaticity).

### 3.2. Spatio-temporal distribution of temperature and soot

The spatio-temporal distribution of temperature and soot in the spray flame for each fuel has been presented in Fig. 9(a–d) and Fig. 10(a–d) respectively. The data shown are from a single injection event but are representative of the trends observed in the previous graphs.

As shown in Fig. 9(a–d), the overall temperature distribution was similar between fuels. During the early soot formation period (1097 μs aSoI), all flames exhibited larger variations in temperature distribution, as the spray flame was not fully developed, and the reactions had not stabilised yet. For all fuels, as the flame developed (2105 μs aSoI), the temperature fields in the central line-of-sight region appeared to be more uniformly distributed but with some randomly distributed regions showing slightly higher temperatures near the flame periphery. After the flame impinged on the wall (>3225 μs aSoI), the flame regions nearer to the wall experienced slightly lower flame temperatures due to heat transfer between the flame and the wall. Towards the end of combustion (>4345 μs aSoI), localised high and low temperature regions were observed in the flame as a result of the consumption of the last pockets of injected fuel, which had a momentum deficit compared to the spray. The temperature variations could also be associated with the late stage oxidation of soot, which oxidised in a rela-

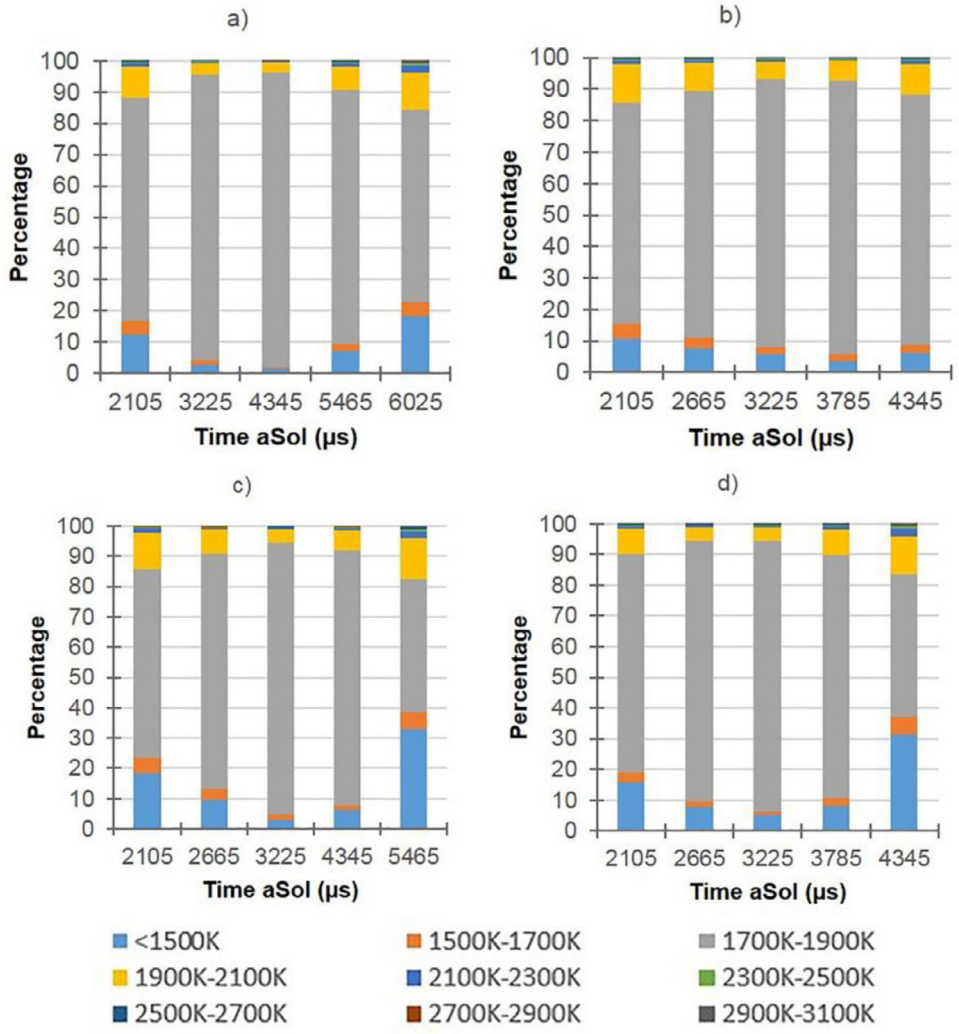


**Fig. 11..** Percentage ranges of the flame temperature. The data are an average of at least seven injection events. (a) Diesel, (b) 2-octanone, (c) 1-octanol, (d) hexyl acetate.

tively oxygen-depleted environment. The overall effect of these final stages (>4345 µs aSoI) was a decrease in the average flame temperature as portrayed in Fig. 6, with strong fluctuations around the mean due to the consumption of the last pockets of fuel and to the oxidation of soot in an environment with relatively less ambient oxygen available for soot oxidation.

The soot distributions for diesel and the oxygenates are shown in Fig. 10(a–d). During the early combustion stages (1097 µs aSoI), soot was observed mainly at the centre and at the tip of the flame for all fuels. As discussed in previous sections, it seems that pyrolysis at these high temperatures prompted soot to form earlier for the oxygenates. As the flame developed and the combustion stabilised, differences in sooting tendencies between fuels became apparent. As shown previously in Fig. 7 and as shown in Fig. 10, the oxygenates produced overall much less soot than diesel. For diesel at 2105 µs aSoI, high sooting regions were observed in the central region and at the tip of the flame due to the presence of various aromatics and long carbon chain compounds that tend to produce a rich pool of soot precursors. For the same point in time, for octanone, higher sooting regions tend to form towards the tip of the flame in a more localised manner when compared to diesel, with most of the flame remaining with low sooting values, as shown in Fig. 10(b); for octanone, the presence of the C=O group may hinder the formation of soot, thus delaying its onset to a more downstream location. When looking at octanol, there was no significant increase in soot, and no localised high-sooting regions were observed. Similar to octanol, hexyl acetate did not show any increase in soot at this point in time, and all the detectable flame remained with low soot concentration, possibly because of the dilution effects hindering the formation of soot precursors. Alongside this delayed formation, transport and diffusion of the soot to a more downstream location could be playing a role in the accumulation of soot at the tip rather than in the central region of the flame for the acquired line-of-sight data.

As combustion developed, soot formation reached its peak for diesel at around 3225 µs–4345 µs aSoI, and high sooting regions were observed throughout the flame centre and at the flame tip, covering most of the flame. Low soot was observed near the nozzle due to the reaction of the momentum-deficit fuel distributed downstream of the nozzle in this region rich in combustion products. For octanone, at 2665 µs, the localised pocket of high intensity soot observed for the previous time-step covered a wider area, but it remained at the tip of the flame. At 3225 µs, the soot in this region intensified and spread slightly upstream, covering part of the flame with high intensity soot. For octanol, at 2665 µs, high intensity sooting regions were observed at the tip, and at 3225 µs, the sooting intensity increased further, and soot also appeared towards the centre of the flame. For both oxygenates, higher sooting regions appeared first towards the flame tip rather than at the centre of the flame, which remained with low soot con-

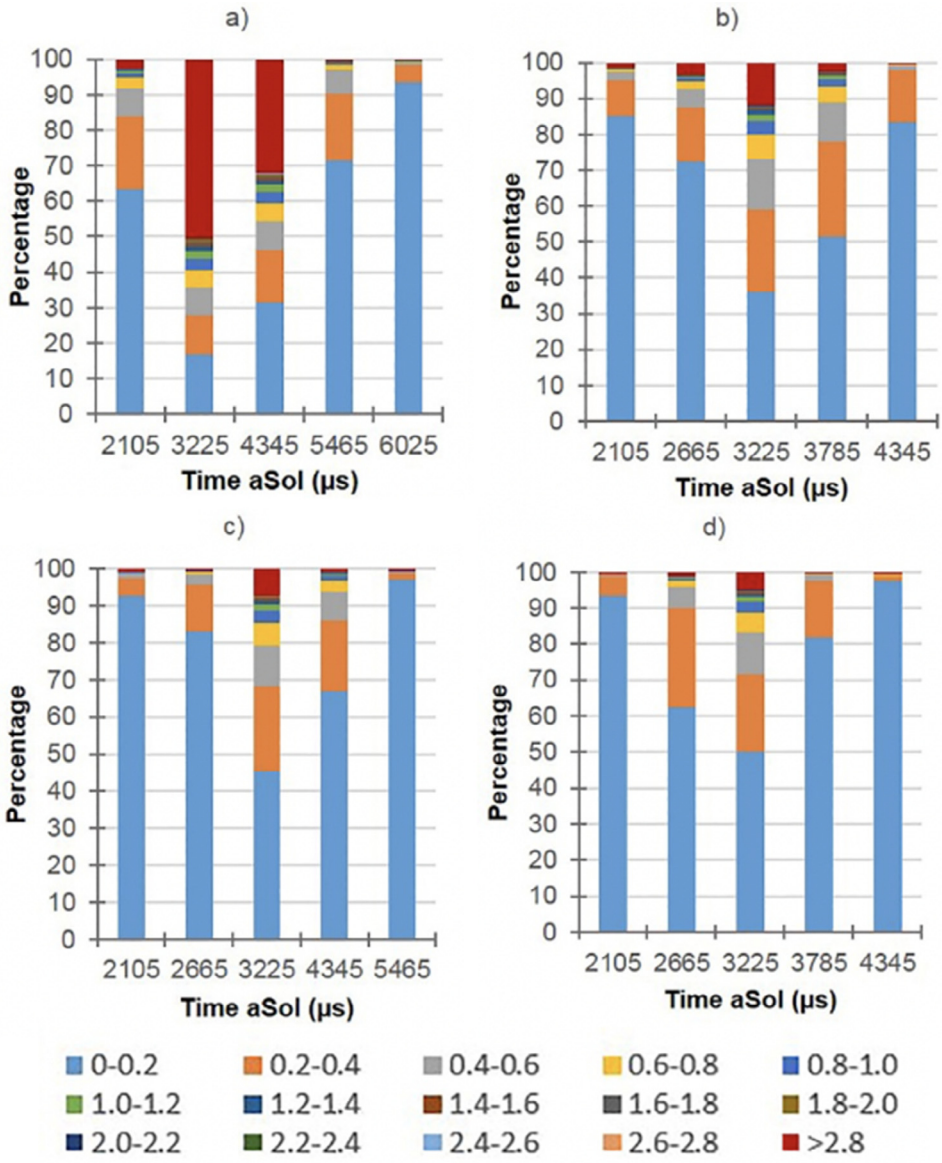


**Fig. 12.** Percentage ranges of the soot distribution. The data are an average of at least 7 injection events. (a) Diesel, (b) 2-octanone, (c) 1-octanol, (d) hexyl acetate.

centration values until the later combustion stages. This could be due to the delay in soot formation and also due to transportation and accumulation of soot precursors at the tip. For hexyl acetate, at 2665 µs only a very localised region at the tip experienced an increase in soot intensity, as similar to octanone and octanol, the formation of soot was hindered until there was sufficient time for the precursors to accumulate. However, in the case of hexyl acetate, high sooting regions remained mostly at the tip. This indicates that for hexyl acetate, soot formation was hindered even in the fuel-rich regions depleted of ambient oxygen.

Towards the later combustion stages (>3225 µs /4345 µs aSoI), high concentrations of soot persisted more for diesel than for any of the oxygenates. High concentrations of soot accumulated at the tip of the flame after it had impinged on the wall and then oxidised relatively slowly. For octanone and octanol, even after the soot had reached its peak, there were still some local high-intensity sooting regions scattered towards the tip of the flame, which persisted longer for octanol than for octanone. For hexyl acetate, after it reached its peak, the soot oxidised promptly, and only low sooting regions remained towards the tip. Overall, for the oxygenates, soot oxidised faster than for diesel and was less persistent during these later combustion stages, which could be due to the different characteristics of the soot produced by the oxygenates.

The percentage of the flame area having different temperature and soot concentrations ranges at different time instants presented in Figs. 9 and 10 are shown in Figs. 11 and 12. These percentages are expressed as an average for the temperature and soot concentration for all injection events at the given time instants, and quantitatively represent the trends observed in the previous figures. The trend of the temperature variation in the spray flame remained fairly constant between all fuels. During the early stages of combustion (2105 µs aSoI), about 10–18% of the flame had regions with temperatures below 1500 K and about 8–12% of the flame had regions with temperatures above 1900 K. During the subsequent combustion stages (between 2665 µs and 3225 µs/4345 µs aSoI), over 85% of the spray flame had a uniform temperature distribution between 1700 K and 1900 K for all fuels. Towards the later combustion stages (>3225 µs/4345 µs aSoI), low regions of <1500 K and high temperature regions of >1900 K were observed to increase, covering around 6–32% and 11–18% of the flame, respectively.

The percentages of the soot distribution in the spray flame are presented in Fig. 12, which shows the extent of soot formation and oxidation for the different fuels. It is interesting to note that these differences in soot formation and oxidation were observed under relatively similar average flame temperatures, which indicates that soot formation and oxidation processes are at least partly dependent on the physio-chemical fuel properties. During the early stages of combustion (2105 μs aSoI), most of the flame had very low soot concentration values of less than 0.2, ranging from 85% to 94% for the oxygenate flames and to a lesser extent of 63% for the diesel flame. This shows that soot precursors formed and accumulated faster for diesel, which resulted in a higher percentage of higher KL values during the early combustion stages. As combustion developed (between 2665 μs and 3225 μs/4345 μs aSoI), diesel had a wider range of KL values than any of the oxygenates, indicating that soot accumulated and formed at more varied rates. For the oxygenates, over 50% of the flame remained at KL values less than 0.4, as soot formation was suppressed during the earlier combustion stages and thus less soot nucleation sites were available for soot to grow.

During these peak sooting points, besides diesel, the largest percentage of higher KL values was observed for octanone, where 41% of the flame area had KL values greater than 0.4. This was followed by octanol, where 32% of the flame area had KL values greater than 0.4 and by hexyl acetate, where 29% of the flame area had KL values greater than 0.4. These results also suggest that for the oxygenates studied, the high sooting regions were confined to a smaller flame area. As combustion approached the final stages (>3225 μs/4345 μs aSoI), for diesel, the high sooting regions did not oxidise as promptly as for the other oxygenates. For hexyl acetate, it was seen that after the peak sooting value was reached, soot oxidised quickly and by a time of 4345 μs aSoI, around 97% of the flame area had KL values less than 0.2. For octanone, at a time of 4345 μs aSoI, 83% of the flame area had KL values of less than 0.2, whereas at the same time instant, for octanol only 67% of the flame area had these KL values. This reflects a slower oxidation process for octanol than for the other oxygenates. Overall, hexyl acetate produced less soot than any other fuel and its sooting regions were confined to the tip and to smaller flame areas when compared to other oxygenates. Whilst octanone and octanol had similar soot distributions, octanone had a slightly higher percentage of the flame area having higher KL values than octanol, which was reflected as higher overall mean soot concentration values in Fig. 7.

The results and findings presented in this section revealed that the temperature distribution remained fairly constant for all fuels. However, there were differences not only in the sooting tendencies but also in the soot distribution between C8 oxygenates that can be related to some extent to their moiety.

## 4. Conclusions

The combustion characteristics of C8 oxygenates were studied under diesel engine-like conditions using the two-colour pyrometry system coupled with high-speed imaging. The aims were: to characterise the combustion and sooting properties of four C8 oxygenated fuels, to study the spatio-temporal development of soot and temperature in the flames, to determine the relative sooting propensity of each oxygenate, and finally, to provide preliminary hypotheses on the potential decomposition routes. The fuels were injected at high ambient temperature conditions to minimise premixing differences between them, and to study primarily the effect of fuel moiety on sooting propensity. The studies revealed that the average flame temperature and the spatial temperature distribution was similar for all fuels throughout the combustion period. During early combustion stages, the temperature steadily increased until it reached a stable value, and then during the late combustion stages, the mean temperature decreased as the fuel and soot pockets were finally consumed.

The formation and oxidation of soot varied between the fuels, with diesel having the highest soot formation rate. For the same amount of injected fuel mass, for the oxygenates, octanone produced the highest amount of soot followed by octanol and hexyl acetate. Though the oxygenate moiety did seem to have an effect on overall soot reduction, for the conditions studied, it was found that the effect of decreasing the carbon backbone chain length, increasing saturation and eliminating aromatics from the fuel composition had more effect on soot reduction than the moiety itself. Under the high pressure injection and ambient temperature conditions the average sooting tendency increased in the order of: ester<aldehyde~alcohol<ketone<diesel.

The spatial distribution and the development of soot in the spray flame were different between the fuels. For diesel, high soot concentration regions formed in the central line-of-sight regions of the flame and at the tip of the flame. For octanone and octanol, high soot concentration regions appeared first at the tip and then in some instances at the central regions. For hexyl acetate, the high soot concentration regions appeared and remained mostly at the tip. For the oxygenates studied, the overall sooting propensity was smaller than for diesel, which makes them potential drop-in fuels to aid on the reduction of soot emissions.

## Declaration of Conflict of Interest

The authors declare that they have no known competing financial interests or personal relationships that could have appeared to influence the work reported in this paper.

## Acknowledgements

This work was supported financially by the Engineering and Physical Science Research Council (EPSRC) and is gratefully acknowledged.

## References

[1] T.V. Johnson, Diesel Particulate Filter Technology, SAE International, 2007.
[2] A. La Rocca, J. Campbell, M.W. Fay, O. Orhan, Soot-in-oil 3D volume reconstruction through the use of electron tomography: an introductory study, Tribol. Lett. 61 (2016) 1–11, doi:10.1007/s11249-015-0625-z.
[3] C.J. Mueller, G.C. Martin, Effects of oxygenated compounds on combustion and soot evolution in a DI diesel engine:broadband natural luminosity imaging, SAE (2020), doi:10.4271/2002-01-1631.
[4] W. Park, S. Park, R.D. Reitz, E. Kurtz, The effect of oxygenated fuel properties on diesel spray combustion and soot formation, Combust. Flame 180 (2017) 276–283, doi:10.1016/j.combustflame.2016.02.026.
[5] P. Pepiot-Desjardins, H. Pitsch, R. Malhotra, S.R. Kirby, A.L. Boehman, Structural group analysis for soot reduction tendency of oxygenated fuels, Combust. Flame 154 (2008) 191–205, doi:10.1016/j.combustflame.2008.03.017.
[6] E.J. Barrientos, M. Lapuerta, A.L. Boehman, Group additivity in soot formation for the example of C-5 oxygenated hydrocarbon fuels, Combust. Flame 160 (2013) 1484–1498, doi:10.1016/j.combustflame.2013.02.024.
[7] N. Miyamoto, H. Ogawa, N.M. Nururn, K. Obata, T. Arima, Smokeless, low NOx, high thermal efficiency, and low noise diesel combustion with oxygenated agents as main fuel, SAE (1998), doi:10.1098/rstb.2008.0317.
[8] Z. Zheng, X. Wang, L. Yue, H. Liu, M. Yao, Effects of six-carbon alcohols, ethers and ketones with chain or ring molecular structures on diesel low temperature combustion, Energy Convers. Manag 124 (2016) 480–491, doi:10.1016/j.enconman.2016.07.057.
[9] R. Lemaire, D. Lapalme, P. Seers, Analysis of the sooting propensity of C-4 and C-5 oxygenates: comparison of sooting indexes issued from laser-based experiments and group additivity approaches, Combust. Flame 162 (2015) 3140–3155, doi:10.1016/j.combustflame.2015.03.018.
[10] Z. Hong, D.F. Davidson, S.S. Vasu, R.K. Hanson, The effect of oxygenates on soot formation in rich heptane mixtures: a shock tube study, Fuel 88 (2009) 1901–1906, doi:10.1016/j.fuel.2009.04.013.
[11] C.S. McEnally, L.D. Pfefferle, Sooting tendencies of oxygenated hydrocarbons in laboratory-scale flames, Environ. Sci. Technol. 45 (2011) 2498–2503.
[12] C.K. Westbrook, W.J. Pitz, H.J. Curran, Chemical kinetic modeling study of the effects of oxygenated hydrocarbons on soot emissions from diesel engines, J. Phys. Chem. A 110 (2006) 6912–6922, doi:10.1021/jp056362g.

[13] Z. Gao, X. Zou, Z. Huang, L. Zhu, Predicting sooting tendencies of oxygenated hydrocarbon fuels with machine learning algorithms, Fuel 242 (2019) 438–446, doi:10.1016/j.fuel.2019.01.064.
[14] B. Kerschgens, L. Cai, H. Pitsch, B. Heuser, S. Pischinger, Di-n-buthylether, n-octanol, and n-octane as fuel candidates for diesel engine combustion, Combust. Flame 163 (2016) 66–78, doi:10.1016/j.combustflame.2015.09.001.
[15] B. Heuser, T. Laible, M. Jakob, F. Kremer, S. Pischinger, C8-oxygenates for clean diesel combustion, SAE (2014), doi:10.4271/2014-01-1253.
[16] L. Cai, A. Sudholt, D.J. Lee, F.N. Egolfopoulos, H. Pitsch, C.K. Westbrook, S.M. Sarathy, Chemical kinetic study of a novel lignocellulosic biofuel: Di-n-butyl ether oxidation in a laminar flow reactor and flames, Combust. Flame 161 (2014) 798–809, doi:10.1016/j.combustflame.2013.10.003.
[17] S. Thion, C. Togbé, Z. Serinyel, G. Dayma, P. Dagaut, A chemical kinetic study of the oxidation of dibutyl-ether in a jet-stirred reactor, Combust. Flame 185 (2017) 4–15, doi:10.1016/j.combustflame.2017.06.019.
[18] E. Koivisto, N. Ladommatos, M. Gold, The influence of various oxygenated functional groups in carbonyl and ether compounds on compression ignition and exhaust gas emissions, Fuel 159 (2015) 697–711, doi:10.1016/j.fuel.2015.07.018.
[19] J. Julis, W. Leitner, Synthesis of 1-octanol and 1,1-dioctyl ether from biomass-derived platform chemicals, Angew. Chem. – Int. Ed. 51 (2012) 8615–8619, doi:10.1002/anie.201203669.
[20] R. Shi, F. Wang, X. Mu, Y. Li, X. Huang, W. Shen, MgO-supported Cu nanoparticles for efficient transfer dehydrogenation of primary aliphatic alcohols, Catal. Commun. 11 (2009) 306–309, doi:10.1016/j.catcom.2009.10.023.
[21] M. Karra-Châabouni, H. Ghamgui, S. Bezzine, A. Rekik, Y. Gargouri, Production of flavour esters by immobilized Staphylococcus simulans lipase in a solvent-free system, Process Biochem. 41 (2006) 1692–1698, doi:10.1016/j.procbio.2006.02.022.
[22] J.C. Jones, Hydrocarbons – Physical Properties and Their Relevance to Utilisation, Ventus Publishing ApS, 2012.
[23] H. Song, K. Quinton, Z. Peng, H. Zhao, N. Ladommatos, Effects of oxygen content of fuels on combustion and emissions of diesel engines, Energies 9 (2016) 28, doi:10.3390/en9010028.
[24] T.N. Patro, D.A. Larue, Alternate fueled powertrain – an insight into its combustion related NVH issues, SAE Tech. (1992), doi:10.4271/1999-01-1758.
[25] F. Harnisch, I. Blei, T.R. Dos Santos, M. Möller, P. Nilges, P. Eilts, U. Schröder, From the test-tube to the test-engine: assessing the suitability of prospective liquid biofuel compounds-Supplementary information, RSC Adv. 3 (2013) 9594–9605, doi:10.1039/c3ra40354h.
[26] C.C. Chen, H.J. Liaw, Y.Y. Kuo, Prediction of autoignition temperatures of organic compounds by the structural group contribution approach, J. Hazard. Mater. 162 (2009) 746–762, doi:10.1016/j.jhazmat.2008.05.137.
[27] J. Fu, J. Shu, Z. Zhao, J. Liu, F. Zhou, Comparative analysis of soot formation processes of diesel and ABE (Acetone-Butanol-Ethanol) based on CFD coupling with phenomenological soot model, Fuel 203 (2017) 380–392, doi:10.1016/j.fuel.2017.04.108.
[28] Y. Marcus, Structural aspects of water in 1-octanol, J. Solut. Chem. 19 (1990) 507–517, doi:10.1007/BF00650383.
[29] D.J.G. Marino, P.J. Peruzzo, G. Krenkel, E.A. Castro, QSPR modeling of heat of formation and heat of vaporization of aliphatic ketones by means of electrotopological indices, Chem. Phys. Lett. 369 (2003) 325–334, doi:10.1016/S0009-2614(02)02023-7.
[30] J.S. Chickos, W.E. Acree, Enthalpies of vaporization of organic and organometallic compounds, 1880–2002, J. Phys. Chem. Ref. Data 32 (2003) 519–878, doi:10.1063/1.1529214.
[31] I. Ruiz-Rodriguez, R. Cracknell, M. Parkes, T. Megaritis, L. Ganippa, Experimental study on the combustion characteristics of high-pressure octanal spray flames, Fuel (2020) 262, doi:10.1016/j.fuel.2019.116596.
[32] R. Pos, M. Avulapati, R. Wardle, R. Cracknell, T. Megaritis, L. Ganippa, Combustion of ligaments and droplets expelled after the end of injection in a multi-hole diesel injector, Fuel 197 (2017) 459–466, doi:10.1016/j.fuel.2017.02.048.
[33] R. Pos, R. Wardle, R. Cracknell, L. Ganippa, Spatio-temporal evolution of diesel sprays at the early start of injection, Appl. Energy 205 (2017) 391–398, doi:10.1016/j.apenergy.2017.07.092.
[34] F. Payri, J.V. Pastor, J.M. García, J.M. Pastor, Contribution to the application of two-colour imaging to diesel combustion, Meas. Sci. Technol. 18 (2007) 2579–2598, doi:10.1088/0957-0233/18/8/034.
[35] S. Di Stasio, P. Massoli, Influence of the soot property uncertainties in temperature and volume-fraction measurements by two-colour pyrometry, Meas. Sci. Technol. 5 (1994) 1453–1465, doi:10.1088/0957-0233/5/12/006.
[36] N. Ladommatos, H. Zhao, A guide to measurement of flame temperature and soot concentration in diesel engines using the two-colour method part I: principles, SAE Tech. Pap. 941957 (1994), doi:10.4271/941956.
[37] H.C. Hottel, F.P. Broughton, Determination of true temperature and total radiation from luminous gas flames: use of special two-color optical pyrometer, Ind. Eng. Chem. – Anal. Ed. 4 (1932) 166–175, doi:10.1021/ac50078a004.
[38] T. Kamimoto, N. Uchida, T. Aizawa, K. Kondo, T. Kuboyama, Diesel flame imaging and quantitative analysis of in-cylinder soot oxidation, Int. J. Engine Res. 18 (2017) 422–435, doi:10.1177/1468087416629282.
[39] Y. Matsui, T. Kamimoto, S. Matsuoka, Formation and oxidation processes of soot particulates in a D. I. diesel engine—An experimental study via the two–color method, SAE International, 1982.
[40] T. Urdan, Statistics in Plain English, third ed., Taylor & Francis, New York, 2011.
[41] D.R. Tree, K.I. Svensson, Soot processes in compression ignition engines, Prog. Energy Combust. Sci. 33 (2007) 272–309, doi:10.1016/j.pecs.2006.03.002.
[42] O.I. Smith, Fundamentals of soot formation in flames with application to diesel engine particulate emissions, Prog. Energy Combust. Sci. 7 (1981) 275–291, doi:10.1016/0360-1285(81)90002-2.
[43] Ö.L. Gülder, Effects of oxygen on soot formation in methane, propane, and n-butane diffusion flames, Combust. Flame 101 (1995) 302–310, doi:10.1016/0010-2180(94)00217-G.
[44] H.S. Hura, I. Glassman, Soot formation in diffusion flames of fuel/oxygen mixtures, Symp. Combust. 22 (1989) 371–378, doi:10.1016/S0082-0784(89)80043-8.
[45] J.E. Dec, C. Espey, Chemiluminescence imaging of autoignition in a DI diesel engine, SAE (1998), doi:10.4271/982685.
[46] C.J. Mueller, W.J. Pitz, L.M. Pickett, G.C. Martin, D.L. Siebers, C.K. Westbrook, Effects of oxygenates on soot processes in DI diesel engines: experiments and numerical simulations, SAE (2003), doi:10.4271/2003-01-1791.
[47] L.M. Pickett, D.L. Siebers, Fuel effects on soot processes of fuel jets at DI diesel conditions, SAE (2003), doi:10.4271/2003-01-3080.
[48] J. Benajes, J. Martín, A. García, D. Villalta, A. Warey, In-cylinder soot radiation heat transfer in direct-injection diesel engines, Energy Convers. Manag 106 (2015) 414–427, doi:10.1016/j.enconman.2015.09.059.
[49] J. Eismark, M. Balthasar, A. Karlsson, T. Benham, M. Christensen, I. Denbratt, Role of late soot oxidation for low emission combustion in a diffusion-controlled, high-EGR, heavy duty diesel engine, SAE Tech. Pap. 4970 (2009) 1–15, doi:10.4271/2009-01-2813.
[50] Andersson Ö., J. Somhorst, R. Lindgren, R. Blom, M. Ljungqvist, Development of the euro 5 combustion system for volvo cars' 2.4.I diesel engine, SAE Tech. Pap. (2009), doi:10.4271/2009-01-1450.
[51] M. Pelucchi, C. Cavallotti, E. Ranzi, A. Frassoldati, T. Faravelli, Relative reactivity of oxygenated fuels: alcohols, aldehydes, ketones, and methyl esters, Energy Fuels 30 (2016) 8665–8679, doi:10.1021/acs.energyfuels.6b01171.
[52] J.A. Miller, C.F. Melius, Kinetic and thermodynamic issues in the formation of aromatic compounds in flames of aliphatic fuels, Combust. Flame 91 (1992) 21–39, doi:10.1016/0010-2180(92)90124-8.
[53] J. Badra, A.E. Elwardany, F. Khaled, S.S. Vasu, A. Farooq, A shock tube and laser absorption study of ignition delay times and OH reaction rates of ketones: 2-Butanone and 3-buten-2-one, Combust. Flame 161 (2014) 725–734, doi:10.1016/j.combustflame.2013.10.001.
[54] S. Yoon, S. Lee, S. Chung, Effect of mixing methane, ethane, propane and propene on the synergistic effect of PAH and soot formation in ethylene-base counterflow diffusion flames, Proc. Combust. Inst. 30 (2005) 1417–1424, doi:10.1016/j.proci.2004.08.038.
[55] U. Burke, J. Beeckmann, W.A. Kopp, Y. Uygun, H. Olivier, K. Leonhard, H. Pitsch, K.A. Heufer, A comprehensive experimental and kinetic modeling study of butanone, Combust. Flame 168 (2016) 296–309, doi:10.1016/j.combustflame.2016.03.001.
[56] J.M. Hudzik, J.W. Bozzelli, Thermochemistry and bond dissociation energies of ketones, J. Phys. Chem. A. 116 (2012) 5707–5722, doi:10.1021/jp302830c.
[57] S.J. Blanksby, G.B. Ellison, Bond dissociation energies of organic molecules, Acc. Chem. Res. 36 (2003) 255–263, doi:10.1021/ar020230d.
[58] L. Cai, Y. Uygun, C. Togbé, H. Pitsch, H. Olivier, P. Dagaut, S.M. Sarathy, An experimental and modeling study of n-octanol combustion, Proc. Combust. Inst. 35 (2015) 419–427, doi:10.1016/j.proci.2014.05.088.
[59] C. Russo, A. D'Anna, A. Ciajolo, M. Sirignano, The effect of butanol isomers on the formation of carbon particulate matter in fuel-rich premixed ethylene flames, Combust. Flame 199 (2019) 122–130, doi:10.1016/j.combustflame.2018.10.025.
[60] L.S. Tran, B. Sirjean, P.A. Glaude, R. Fournet, F. Battin-Leclerc, Progress in detailed kinetic modeling of the combustion of oxygenated components of biofuels, Energy 43 (2012) 4–18, doi:10.1016/j.energy.2011.11.013.
[61] S.M. Sarathy, P. Oßwald, N. Hansen, K. Kohse-Höinghaus, Alcohol combustion chemistry, Prog. Energy Combust. Sci. 44 (2014) 40–102, doi:10.1016/j.pecs.2014.04.003.
[62] J. Abboud, J. Schobing, G. Legros, A. Matynia, J. Bonnety, V. Tschamber, A. Brillard, G. Leyssens, P. Da Costa, Impacts of ester's carbon chain length and concentration on sooting propensities and soot oxidative reactivity: application to Diesel and Biodiesel surrogates, Fuel 222 (2018) 586–598, doi:10.1016/j.fuel.2018.02.103.
[63] C.K. Westbrook, W.J. Pitz, P.R. Westmoreland, F.L. Dryer, M. Chaos, P. Osswald, K. Kohse-Höinghaus, T.A. Cool, J. Wang, B. Yang, N. Hansen, T. Kasper, A detailed chemical kinetic reaction mechanism for oxidation of four small alkyl esters in laminar premixed flames, Proc. Combust. Inst. 32 (2009) 221–228, doi:10.1016/j.proci.2008.06.106.
[64] H.J. Seong, A.L. Boehman, Studies of soot oxidative reactivity using a diffusion flame burner, Combust. Flame 159 (2012) 1864–1875, doi:10.1016/j.combustflame.2012.01.009.
[65] R.L. Vander Wal, C.J. Mueller, Initial investigation of effects of fuel oxygenation on nanostructure of soot from a direct-injection diesel engine, Energy Fuels 20 (2006) 2364–2369, doi:10.1021/ef060201.
[66] N.S.I. Alozie, G. Fern, D. Peirce, L. Ganippa, Influence of biodiesel blending on particulate matter (PM) oxidation characteristics, SAE. (2017). doi:10.4271/2017-01-0932. Copyright.
[67] R.L. Vander Wal, A.J. Tomasek, Soot nanostructure: dependence upon synthesis conditions, Combust. Flame 136 (2004) 129–140, doi:10.1016/j.combustflame.2003.09.008.
[68] J Yanowitz, M Ratcliff, R McCormick, J Taylor, M Murphy, Compendium of Experimental Cetane Numbers, NREL, 2014.